KEK Preprint 98-187
DPNU 98-42
KUDP 98-01
TUAT-HEP 98-02
KINDAI-HEP 98-01
November 1998
H

Designing of Stereo-Wire Geometry for a Long Cylindrical Drift Chamber with Small Jet Cells

N.Khalatyan[a], *K.Fujii*[a], *H.Okuno*[a], *T.Abe*[c1], *K.Hoshina*[b], *Y.Kato*[e], *Y.Kurihara*[a], *H.Kuroiwa*[b], *T.Matsui*[a], *O.Nitoh*[b], *A.Sugiyama*[c], *K.Takahashi*[b], *T.Watanabe*[d], *T.Yoshida*[a],

[a] High Energy Accelerator Research Organization(KEK), Tsukuba, 305-0801, Japan
[b]Tokyo University of Agriculture and Technology, Tokyo 184-8588, Japan
[c]Department of Physics, Nagoya University, Nagoya 464-8602, Japan
[d]Kogakuin University, Tokyo 163-8677, Japan
[e]Kinki University, Osaka, 577-8502, Japan

Abstract

Common problems in designing stereo-wire geometry for a long cylindrical drift chamber with small jet cells are described and possible ways to approach them are discussed in detail. Among these problems, special emphasis is put on the surface field variation along an anode wire due to the geometrical deformation of the cell structure. Also estimated is the surface field variation due to electrostatic and gravitational sags, based on the sags measured for a 4.6 m-long test chamber. These field variations are translated into gain variation along the stereo wires and used to constrain the stereo geometry.

[1]Now at SLAC, California, USA

1 Introduction

One of the most striking features of experiments at a future linear e^+e^- collider such as JLC[1] is the novel possibility of recognizing all physics processes in terms of fundamental particles (leptons, quarks, and gauge bosons). This involves explicit reconstructions of heavy unstable particles such as W, Z, and t through jet invariant-mass measurements. In order to achieve the best attainable jet invariant-mass resolution, it is crucial to make maximum use of information from a central tracking device as well as that from calorimetry. Essential is thus good track-cluster matching capability to avoid double counting, not to mention a high momentum resolution with a wide angular acceptance. A large cylindrical drift chamber with small jet cells is a candidate central tracking device to fulfill these requirements. From the track-cluster matching point of view, what we are concerned most is track extrapolation errors, which depend on both r-ϕ and z resolutions. Improvement of the latter necessitates introduction of stereo wires, since the z resolution in charge division or time difference readout is typically 1 % of the wire length or worse, which is a few cm in the linear collider use.

In this paper we describe common problems in designing stereo-wire geometry for a long cylindrical drift chamber with small jet cells and discuss possible ways to approach them in detail. The surface field variation along an anode wire is one of the most important among these problems, and deserves special attention. Possible sources of such a field variation include (1) the geometrical deformation of the cell structure as a function of z (the coordinate along the chamber axis) due to stereo geometry, and (2) that due to electrostatic and gravitational sags. These field variations are estimated through explicit electric field calculations using the chamber simulation program GARFIELD[3]. As for the second source, we use the electrostatic and gravitational sags directly measured for a 4.6 m-long test chamber[4]. The estimated field variations are translated into gain variation along the anode wires using the gas gain data taken for this purpose. We then use this gain variation as a key parameter to constrain the stereo geometry.

The paper is organized as follows. We begin with a general description of geometrical parameters that determine the configuration of a cylindrical drift chamber with axial and stereo layers of small jet cells, and then outline the decision process for these parameters in section 2. Taking a candidate central tracker for JLC as an example, we will demonstrate the procedure in the following sections. Finally section 6 summarizes our results and concludes this paper.

2 Outline of Geometrical Parameters Decision Process

The parameters that determine the geometrical configuration of a small-jet-cell cylindrical drift chamber can be classified into two groups: (1) global parameters that specify the size and layout of axial and stereo super-layers, and (2) local parameters that describe the geometry of a jet cell in each super-layer. The first class includes the length, the inner and

outer radii, and the stereo angle[2] of each super-layer. If there is a layer of shielding wires between adjacent super-layers, its radius and stereo angle also belong to this class. The parameters in the second class are, essentially, the relative locations of wires that comprise a single jet cell, and determine the local properties of the chamber. These parameters are optimized to achieve performance goals such as required spatial resolution, two-hit separation capability, etc, together with other non-geometrical parameters including wire high voltages, gas mixture, magnetic field, and so on. Detailed discussions on decision process for these parameters are beyond the scope of this paper and will not be covered unless necessary in the context of stereo geometry determination.

2.a Basic Chamber Parameters in Terms of Physics Requirements

Now let us outline a typical parameters decision process. The chamber performance goals required by physics of interest are often expressed in terms of transverse momentum resolution, dip angle resolution, two-track separation capability, and polar angle coverage. The transverse momentum resolution σ_{p_T} is approximately given by the following formula[2]:

$$\frac{\sigma_{p_T}}{p_T} \simeq \sqrt{\left(\frac{\alpha'\sigma_{r\phi}}{Bl^2}\right)^2 \left(\frac{720}{n+4}\right) {p_T}^2 + \left(\frac{\alpha' C}{Bl}\right)^2 \left(\frac{10}{7}\left(\frac{X}{X_0}\right)\right)}, \tag{2.1}$$

where

$$\begin{cases} \sigma_{r\phi} & = & \text{spatial resolution in the } r\text{-}\phi \text{ plane per wire} \\ n & = & \text{the number of sampling points} \\ \alpha' & = & 333.56 \ (\text{cm} \cdot \text{T} \cdot \text{GeV}^{-1}) \\ C & = & 0.0141 \ (\text{GeV}) \\ (X/X_0) & = & \text{thickness measured in radiation length units} \\ l & = & \text{lever arm length (cm)} \\ B & = & \text{magnetic field (T)} \end{cases} . \tag{2.2}$$

The number of sampling points is practically determined by the lever arm length and the minimum possible wire-to-wire distance. The best result is thus expected for the largest possible B field and lever arm length with the smallest possible spatial resolution. Since the required polar angle coverage determines the wire length when the lever arm length and the radial position of the innermost wires are given, the lever arm length is limited by the maximum possible wire length for stable chamber operation[3]. The B field essentially

[2]Strictly speaking, stereo angle, which is defined as the wire angle measured from the axial direction, slightly varies even within a single jet cell: it increases linearly with the radial position of a wire. As discussed later, the stereo angle of the innermost wire is the most important in deciding the stereo geometry.

[3]There are some external constraints on the radial positions of the inner- and outermost wires: the radial position of the innermost wires is constrained, in the case of the present JLC design, by the size of the support tube for the final focusing quadripole magnets that reside in the detector system. The radial position of the outermost wires has to be consistent with the surrounding barrel calorimeter.

determines the Lorentz angle given a chamber gas mixture[5] and, if a tilted cell structure is adopted, it imposes a limit on the two-hit separation capability. There will also be a technical limit to the maximum possible B field attainable with a superconducting solenoid from the mechanical strength and the stored energy to be released upon quench.

On the other hand, the dip angle resolution $\sigma_{\tan\lambda}$ can be written in the form[2]:

$$\sigma_{\tan\lambda} \simeq \sqrt{\left(\frac{\sigma_z}{l}\right)^2 \left(\frac{12}{n}\right) + (1+\tan^2\lambda)\left(\frac{C}{p_T}\right)^2 \left(\frac{13}{35}\left(\frac{X}{X_0}\right)\right)}, \tag{2.3}$$

where σ_z is the spatial resolution per wire in the axial direction which is given by

$$\sigma_z = \sigma_{r\phi}/\tan\alpha \tag{2.4}$$

in the case of stereo wires with a stereo angle α. Provided that l and B are predetermined by the requirement on the transverse momentum resolution, the only free parameter left here is the stereo angle. Apparently the larger the stereo angle becomes the better the dip angle resolution. There are, however, various restrictions to the stereo angle which are the main topics of this paper.

The two-hit separation capability is controlled by the width of a sense wire signal which is determined by the arrival time distribution of track electrons, space charge effects in the avalanche formation, and the subsequent readout electronics. Apart from the optimization of the readout electronics, appropriate choices of the drift line configuration and chamber gas are thus important. In any case, the relation of the two-hit separation capability issue to the stereo geometry is at most indirect and can be treated separately as a problem concerning local properties of the chamber[6].

2.b Global Stereo-Geometrical Parameters

At this point we have a rough idea about basic parameters describing the chamber: the inner and outer radii, the length, the number of sampling points, and the $r\phi$ spatial resolution per wire. In order to decide the stereo geometry, we further need to know the super-layer layout of the chamber and problems introduced by the use of finite stereo angles. A stereo layer can be formed by rotating the end point of each wire belonging to this layer by a small angle ($\Delta\phi$) with the other end point fixed. As illustrated in Fig.1, the stereo angle α is related to $\Delta\phi$ and the wire length (L) through

$$\begin{aligned} \alpha &= \tan^{-1}\left(\frac{2r(z=\pm L/2)}{L}\sin\left(\frac{\Delta\phi}{2}\right)\right) \\ &\simeq \frac{r(z=\pm L/2)}{L}\cdot\Delta\phi, \end{aligned} \tag{2.5}$$

which suggests α being r-dependent even within a single stereo jet cell as mentioned earlier.

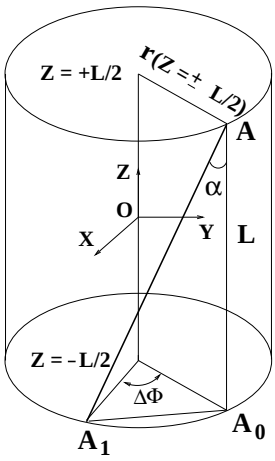

Figure 1: 3-dimensional view of a single stereo wire.

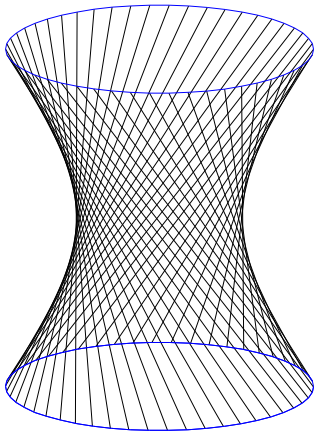

Figure 2: Formation of a hyperboloidal surface due to stereo wires.

The otherwise cylindrical surface of this wire layer turns into a hyperboloidal surface as shown in Fig.2. As a result, both the azimuthal angle and the radial position of the stereo wire becomes z-dependent:

$$\begin{aligned} \phi(z) &= \phi(z=0) + \tan^{-1}\left[\left(\frac{2z}{L}\right)\tan\left(\frac{\Delta\phi}{2}\right)\right] \\ r(z) &= \sqrt{\left(r(z=0)\right)^2 + \left(z\tan\alpha\right)^2} \\ &= \sqrt{\left(r(z=\pm L/2)\right)^2 + (z^2 - (L/2)^2)\tan^2\alpha}, \end{aligned} \tag{2.6}$$

where z is measured from the middle of the chamber along the chamber axis [4].

This inhomogeneity distorts the electric field to some extent and limits the maximum possible stereo angle, thereby restricting the z resolution σ_z. Fig.3 demonstrates how a single stereo cell structure deforms as one moves from one endplate to the other. This z-dependent geometrical deformation of the stereo cell is parametrized by a so called shrink factor and imposes another important restriction on the possible range of stereo angles.

The shrink factor $f(z)$ is defined to be the ratio $A_2B_2(z)/AB(z=\pm L/2)$ in Fig.3

[4]The azimuthal wire position becomes a linear function, and the radial wire position a quadratic function of z measured from the middle of the chamber:

$$\begin{cases} \phi(z) \simeq \phi(z=0) + \left(\frac{\alpha z}{r(z=0)}\right) \\ r(z) \simeq r(z=0) + \frac{1}{2}\left(\frac{(\alpha z)^2}{r(z=0)}\right) \end{cases} \tag{2.7}$$

to the lowest order of αz.

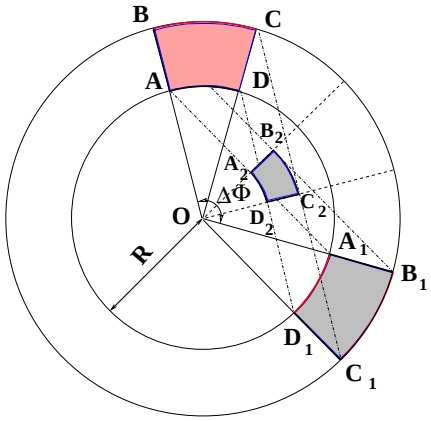

Figure 3: Exaggerated illustration of the stereo-cell formation through rotation by an angle $\Delta\phi$ and its deformation along the wires. $ABCD$ and $A_1B_1C_1D_1$ are the cross sections of a single stereo cell at the end plates ($z = \pm L/2$). $A_2B_2C_2D_2$ is that of the same stereo cell inbetween ($-L/2 < Z < +L/2$).

and is readily derived from Eqs.2.5 and 2.6:

$$\begin{aligned} f(z) &= \frac{r_B(z) - r_A(z)}{r_B(z = \pm L/2) - r_A(z = \pm L/2)} \\ &= \sqrt{1 + \left(\frac{z^2 - (L/2)^2}{L^2}\right) 4\sin^2\left(\frac{\Delta\phi}{2}\right)} \\ &= \frac{\sqrt{R^2 + (z^2 - (L/2)^2)\tan^2\alpha}}{R}, \end{aligned} \tag{2.8}$$

where $R = r(z = \pm L/2)$ and $f(z = \pm L/2) = 1$ by definition.

It is a common practice to use pairs of stereo super-layers (V and U) with alternating stereo angles ($\pm\alpha$) interleaved with axial super-layers (A)[5]. In this case, the inhomogeneity is more serious for the gap between a stereo super-layer (V) and the adjacent axial super-layer (A) just inside. The minimum gap attained at the middle point of the chamber has to be large enough for stable operations of the chamber.

In the following sections, we will illustrate in detail the parameters decision process for a stereo geometry outlined above, taking an example of a possible JLC central tracking system.

[5]The axial super-layers greatly facilitate track finding in the r-ϕ projection, since stereo super-layers alone cannot provide any absolute coordinate before its z coordinate is determined through tracking. There is, however, a logical possibility to do away with axial layers.

3 Illustration of Stereo Geometry Determination

3.a A Possible Central Tracker for JLC

Basic parameters of a possible JLC central tracker read $B = 2\ T$, $r_{in} = 45$ cm, $r_{out} = 230$ cm, $L = 460$ cm, $n = 80$, and $\sigma_{r\phi} = 100\ \mu$m, whose feasibility is the key issue of our on-going R&D[4]. The tracker consists of 6 axial and 10 stereo super-layers, each having 5 anode wires, arranged with increasing r in the following order: $AVUAVUAVUAVUA$, where A, V, and U again denote an axial super-layer, stereo super-layers with stereo angles of $+\alpha$ and $-\alpha$, respectively. The gap between adjacent super-layers is correlated with the stereo angle and is equal to either 4.0 or 5.0 cm at the endplates, depending on its radial location: the U-to-A and the V-to-U gaps are equal to 4.0 cm, while the A-to-V is set at 5.0 cm (see Fig.4)[6].

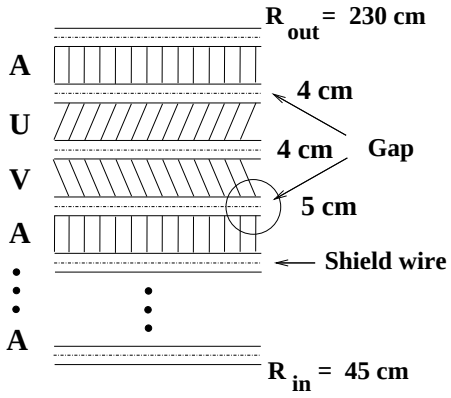

Figure 4: A possible super-layer layout for the central tracking system of the JLC.

In the current design, there is a layer of shielding wires in each gap between adjacent super-layers, in order to electrostatically isolate different super-layers. These shielding wires in a V-to-U gap will have the same stereo angle (α) with the V wires. On the other hand, the shielding wires in A-to-V or U-to-A gaps will have half the stereo angle of the adjacent stereo super-layers ($\pm\alpha/2$). Note also that the stereo angle varies even within a single jet cell, according to Eq.2.5.

3.b Geometrical Limitation to the Stereo Angle

It is already clear that there is a definite geometrical limit to the maximum possible stereo angle: the stereo angle should be small enough to avoid mechanical contact of wires belonging to different layers. The decisive parameter is therefore the minimum

[6] We can further optimize the inter-super-layer distances.

distance between shielding wires and the stereo wires. This is more important for the A-to-V gaps, since an A super-layer stays as a cylinder, while the V super-layer surrounding it shrinks in the middle: it changes its shape to a hyperboloid. In the above mentioned JLC example, the shielding wires are 2.5 cm away from the nearest stereo super-layer (V) at the both wire ends. Along the length of the chamber the distance between the innermost stereo layer belonging to a V super-layer and the adjacent layer of the shielding wires decreases as a quadratic function of z and attains its minimum at $z = 0$.

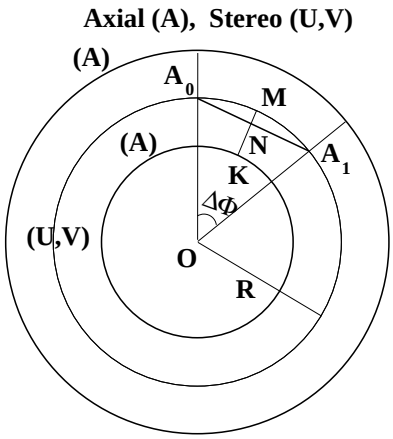

Figure 5: r-ϕ projection of a stereo wire (A_0A_1): MN is the maximum displacement of the stereo wire.

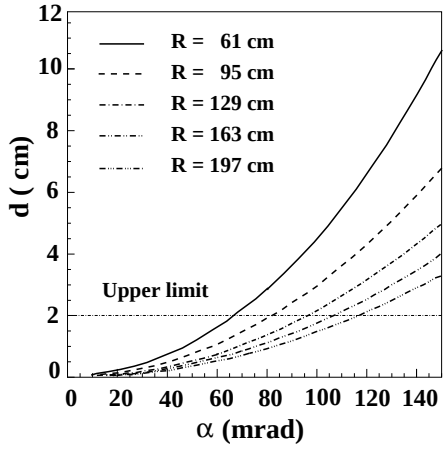

Figure 6: Maximum radial displacement of a stereo wire as a function of the stereo angle for different gaps.

Fig.5 illustrates the $r\phi$ projection (A_0A_1) of a single stereo wire. Then we have

$$A_0A_1 = L \cdot \tan\alpha, \tag{3.9}$$

where the chamber length is $L = 4.6$ m in the JLC example (see Fig.1). MN is the maximum displacement of the stereo wire with respect to its original position on the endplates and corresponds to the middle point ($z = 0$) along the wire:

$$\begin{aligned} MN \equiv d &= r(z = \pm L/2) - r(z = 0) \\ &= R - \sqrt{R^2 - \frac{L^2 \cdot \tan^2\alpha}{4}} \\ &= R\left(1 - \cos\left(\frac{\Delta\phi}{2}\right)\right), \end{aligned} \tag{3.10}$$

where the nominal radius $R = r(z = \pm L/2)$ is the radial position of the stereo wire at the endplates (see Eq.2.6).

In order to prevent the stereo wire from touching any shielding wire, this maximum displacement MN should be less than the nominal distance between the shielding and stereo wires measured at the endplates. The maximum displacement MN, however,

strongly depends on the stereo angle α and the nominal radius R. Given our example central tracker consisting of super-layers having a cell size of 70 mm $\times$ 100 mm (the maximum drift length is thus 5 cm) and being arranged in the $AVUAVUAVUAVUA$ configuration from $r_{in} = 45$ to $r_{out} = 230$ cm, we can easily calculate the radial position of each axial or stereo super-layer as well as the gap between any two neighboring super-layers. Fig.6 plots this maximum displacement MN for each super-layer as a function of stereo angle α. The dashed line is an example of the geometrical upper bound on the maximum displacement (2.0 cm)[7].

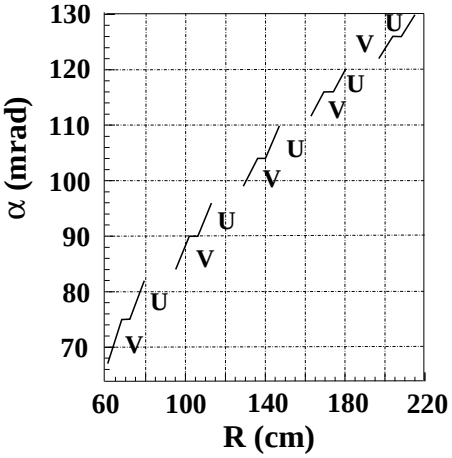

Figure 7: Upper limit of the stereo angle as a function of the radius for all of the 10 stereo super-layers.

Super-layer	R (cm)	α (mrad)	ΔΦ (mrad)
V	61	67	512
U	72	75	483
V	95	84	411
U	106	90	395
V	129	99	356
U	140	104	346
V	163	111	316
U	174	116	309
V	197	122	287
U	208	126	282

Table 1: The radial position (R), stereo angle (α) and rotation angle ($\Delta\phi$) for each stereo super-layer.

Fig.7, on the other hand, shows the upper limit of the stereo angle as a function of the radial position of each super-layer. From these we can read off the geometrical upper limit on the stereo angle for each stereo super-layer. As pointed out above, it should be noted here again that the stereo angle varies even within a single cell according to Eq.2.5: it grows linearly with the radial position. On the other hand, $\Delta\phi$ is constant within a single super-layer.

3.c Z-dependent Geometrical Deformation of Stereo Cells

As shown earlier, the wires belonging to a stereo layer form a hyperboloidal surface. Consequently, any stereo cell shrinks as one moves from an endplate to the middle of the wires. As derived in the previous section, Eq.2.8 tells how the stereo cell shrinks as a function of z:

$$f(z) = \frac{\sqrt{R^2 + \tan^2\alpha\,(z^2 - (L/2)^2))}}{R}. \tag{3.11}$$

[7]The actual maximum allowable displacement here should be decided in terms of electrostatic stability when high voltages are applied. Our experience with a 4.6 m-long test chamber tells us that a distance equal to or greater than 1 cm is enough for wire stability in the case of the present cell design.

In this formula the shrink factor f is a function of z, R, and α. In order to calculate f as a function of z, we use R and α tabulated in Table 1 for each stereo super-layer.

The resultant shrink factor is shown in Fig.8 for all of the 10 (V,U) stereo super-layers.

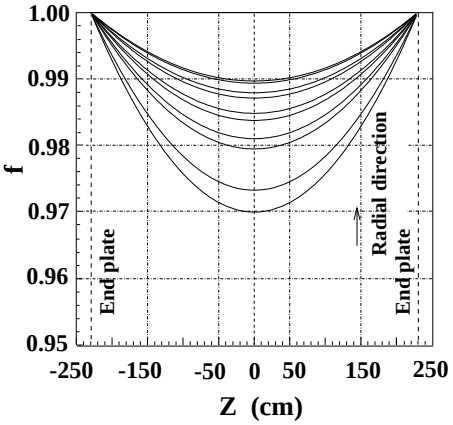

Figure 8: Shrink factor (f) as a function of z for all of the 10 super-layers: from the bottom to the top, the lines correspond to super-layers ordered in the radial direction.

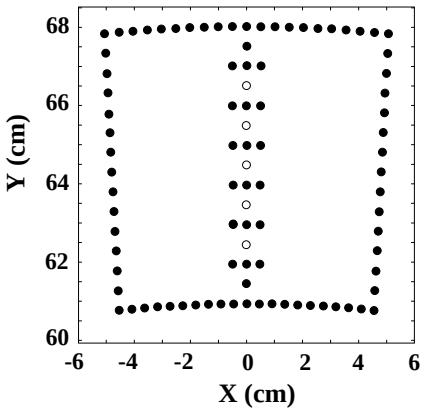

Figure 9: A typical geometry of a single cell: the circles (∘) and (•) correspond to sense and potential wires, respectively.

The variation of the shrink factor $\Delta f/f$ is at most 3 % observed for the innermost stereo super-layer which has $r = 68$ cm and $\alpha = 75$ mrad. The z-dependent geometrical deformation of the stereo cell induces variation of the surface field on the sense wires in it, thereby introducing gain nonuniformity along the wires. We calculated the surface field variation on the sense wires, using the drift chamber simulation program, GARFIELD. The cell structure used in the calculation is shown in Fig.9 whose size depends on the shrink factor f and varies also with the radial position or the super-layer that the cell belongs to.

Fig.10 plots the calculated surface fields against the z coordinate. The maximum variation of the surface field is $\Delta E/E \simeq 0.43$ %.

3.d Surface Field Variation Due to Electrostatic and Gravitational Sags

In addition to the stereo geometry, there is another source of geometrical deformation of the cell structure that is wire sags due to gravitational and electrostatic forces on the wire. These gravitational and electrostatic sags also contribute to the surface field variation and are common to both axial and stereo wires. It suffices to investigate the effects of these wire sags for axial wires only. We, therefore, calculate the surface field variation with GARFIELD, using as input the electrostatic and gravitational sags actually measured as the difference of the wire coordinates at $z = \pm L/2$ (wire ends) and $z = 0$ (mid point)

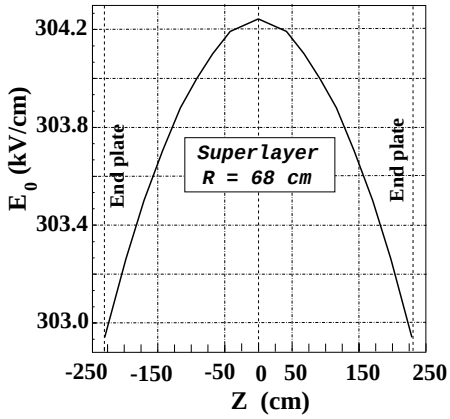

Figure 10: Surface field as a function of z for a sense wire in the innermost stereo super-layer at $r = 68$ cm.

for a 4.6 m-long test chamber[4]. The maximum wire-sag-induced variation of the surface field is $\Delta E_0/E_0 \simeq 1.4$ %. It should be emphasized that the fact that the field variation is comparable with those from the stereo geometry for our example is largely due to the use of Aluminum field wires. We can in principle reduce the field variation from the gravitational and electrostatic sags, by optimizing the wire materials and by stringing these wires with higher tensions. On the other hand, the limitation coming from the stereo geometry is inherent in any stereo chamber and is unavoidable.

4 Gas Gain Variation along Stereo Wires

Now that we know the surface field variation along any wire, we can study its z-dependent gas gain variation and discuss the operation feasibility of the chamber, provided that the relation of the surface field to the gas gain is known. Conversely, the stereo angle should be so determined to make the gain variation acceptable.

We have measured the gas gain for the CO_2(90%)-Isobutane (10%) mixture, by using a single wire proportional counter[7]. This gas mixture is a possible candidate for the JLC central tracker because of its very small diffusion coefficients. The counter is made of an aluminum cathode tube with a 10 mm inner diameter and a gold-plated tungsten anode wire with a 30 μm diameter. For the ^{55}Fe X-rays (5.9 keV) and ^{90}Sr β-rays, the charges collected on the anode within 1 μsec were measured as a function of the applied voltage.

The results of the measurements are depicted in Fig.11, where the collected charge Q is plotted as a function of the anode surface field E_0.

These data are fitted to the following empirical formula:

$$\ln Q = a + bE_0, \tag{4.12}$$

where a and b are the parameters to be determined. From these data, we obtain the

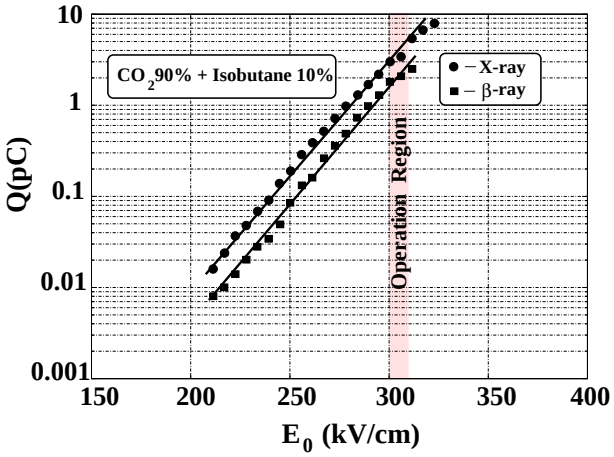

Figure 11: Signal charge as a function of the surface field on a sense wire.

following relation:

$$\frac{\Delta Q}{Q} = (15 \sim 20)\left(\frac{dE_0}{E_0}\right) \tag{4.13}$$

around $E_0 \simeq 300$ kV/cm, where the gas gain is about 10^4.

By combining these results with the surface field variations calculated in the previous subsections, we estimate the gain variation of the stereo wire due to the stereo geometry to be at most 8 % which is acceptable.

The surface field variation due to the wire displacements induced by gravitational and electrostatic forces for our 4.6 m test chamber could give rise to some additional gain variation as large as 25 % at worst. The wire displacements can, however, be reduced by appropriate choices of wire materials enduring higher tensions, a higher gain gas mixture allowing lower high voltages on sense wires, etc. On the other hand, the gas gain variation due to the stereo geometry is irreducible without geometry redesigning.

5 Discussions

In the above, we have been trying to demonstrate a general designing procedure of stereo-wire geometry. In order to make the procedure more transparent and easier to understand, we took a concrete example of a possible central tracker for a future JLC experiment. However, the parameters of the tracker we took as an example are by no means final ones, and need refinements and optimizations: our example of a possible JLC central tracker has $r_{in} = 45$ cm, $r_{out} = 230$ cm, and a cell size of 70 mm $\times$ 100 mm as required by detector performance goals and external constraints from other detector components. The super-layer arrangement ($AVUAVUAVUAVUAVUA$) and inter-super-layer gap sizes (4.0 or 5.0 cm at the endplates) are less well motivated. We discuss below some ideas for further possible improvements.

- The super-layer structure

As mentioned before, the axial super-layers greatly facilitate track finding in the r-ϕ projection, since stereo super-layers alone cannot provide any absolute coordinate before its z coordinate is determined through tracking. Because of this, we assumed throughout this paper the use of axial super-layers together with stereo ones. There is, however, a logical possibility to do away with axial layers. We need more feasibility studies of this point.

- The gaps between adjacent super-layers and the location of shielding wires

  The gaps between adjacent super-layers can be rearranged, for instance, to equalize the minimum distances between any adjacent super-layers, regardless of whether they are A, V, or U-types. We can also allow a larger stereo angle for inner super-layers by giving larger gaps to them.

  The inter-super-layer gaps have single shielding layers. It is now clear from Fig.6 that, by increasing the distance between a stereo super-layer and its adjacent layer of shielding wires, we can increase the stereo angle. This procedure can be particularly important for inner super-layers where stereo angles are less than 100 mrad.

- The shielding layers consisting of stereo wires

  In order to allow a larger displacement of stereo wires in the middle, we proposed to use, for shielding wires, half a stereo angle of the adjacent stereo wires. This also brings more symmetry to gaps between shielding layers and adjacent super-layers.

6 Conclusions

We have outlined a general design procedure for a long cylindrical drift chamber with small jet cells with an emphasis put on the decision process for stereo wires geometry. The procedure was illustrated, taking a concrete example of a possible central tracker for JLC. The surface field variation along an anode wire is one of the decisive factors to determine stereo geometry. We have examined the surface field variation originating from (1) the geometrical deformation of the cell structure as a function of z (the coordinate along the chamber axis) due to stereo geometry, and (2) that due to electrostatic and gravitational sags. These field variations were estimated through explicit electric field calculations using the chamber simulation program GARFIELD[3]. The estimated field variations were translated into gain variation along the anode wires using the gas gain data taken for this purpose and used to constrain the stereo geometry.

Acknowledgments

The authors would like to thank all the members of the JLC physics working group. In particular, they are very grateful to Y.Nakamura for his great contribution in gas gain measurements, N.Ishihara and T.Ohama for useful discussions, and S.Iwata for continuous

encouragements and supports. This work was supported in part by the JSPS Japanese-German Cooperation Program.

References

[1] JLC group, KEK Report 92-16, December,1992.

[2] R.L. Gluckstern, Nucl. Inst. and Meth. **24** (1963) 381, JLC physics group, http://www-jlc.kek.jp/subg/offl/lib/docs/helix_manip.ps.gz.

[3] Veen Hove, A Drift Chamber simulation program GARFIELD, 1994.

[4] S Sudou, N. Khalatyan, Y. Kurihara, T. Abe, K. Fujii, A. Sugiyama, K. Takahashi, T. Watanabe, Nucl. Inst. and Meth. **A383** (1996) 391.

[5] JLC CDC group, a paper on Lorentz angle measurement, in preparation.

[6] JLC CDC group, a paper on two-track separation paper, in preparation.

[7] JLC CDC group, a paper on Gas gain measurement, in preparation.